Mechanisms of nuclear excitation in plasmas

M. R. Harston and J. F. Chemin
Centre d'Etudes Nucléaires de Bordeaux-Gradignan (CENBG), Le Haut Vigneau, BP. 120, F-33175 Gradignan Cedex, France
(Received 2 November 1998)

This paper discusses several mechanisms that could be responsible for nuclear excitation in a plasma of temperature of order 10–100 eV. Four mechanisms discussed in detail are nuclear excitation by a resonant electronic transition from an excited bound state to a lower-lying bound state, nuclear excitation by electron capture from the continuum, photoexcitation, and inelastic electron scattering. Estimates of the rates for these different processes are presented for the excitation of ^{235m}U for which the present experimental data lacks adequate theoretical interpretation. [S0556-2813(99)05004-9]

PACS number(s): 23.20.Nx, 27.90.+b

I. INTRODUCTION

The possibility of exciting nuclear states by coupling of the nucleus to the atomic electron system under the action of a laser field is receiving increased attention with the rapid progress in high intensity laser sources [1]. Indeed, an efficient mechanism for the population of excited nuclear states lies behind any attempt to produce a laser based on a nuclear transition [2]. One system that has been the focus of study is the excitation of the isomeric 1/2+ state of ^{235}U that lies 76.8 ± 0.5 eV above the 7/2- ground state (Fig. 1). Two experiments have given indications of a possible effect of excitation of the isomeric state in a plasma. In the first experiment by a Japanese group [3], a CO_2 laser (1 J, 100 ns) was focused on a natural uranium target, thereby creating a plasma with an electron density near to the cutoff density of 10^{19} electrons cm^{-3}. Excitation of the ^{235m}U isomeric state with an estimated cross section $\simeq 10^{-29}$ cm^2 was observed by counting the conversion electrons from its subsequent decay. A Russian group attempted a similar experiment with a CO_2 laser (5 J, 200 ns) but failed to observe the isomeric state [4,5]. The same group later [5] performed an experiment in which an electron beam of energy 500 keV was incident on a uranium target which was heated to an estimated temperature of 20 eV. The isomeric state, again detected by means of the conversion electrons from its decay, was observed to be produced with an estimated cross section $\simeq 10^{-32} - 10^{-31}$ cm^2. More recently, Bounds and Dyer [6] have investigated nuclear excitation in a ^{235}U plasma created using a low-intensity CO_2 laser to create the plasma with irradiation by a high-intensity ($\simeq 10^{15}$ W cm^{-2}) 700 fs laser at 248 nm. An upper limit for the nuclear excitation probability of 4.0×10^{-5} per 700 fs pulse was reported. The characteristics and results of these experiments are summarized in Table I.

The mechanisms responsible for nuclear excitation of ^{235m}U under the conditions present in experiments [3] and [5] remain uncertain [1]. One mechanism that has been previously discussed [7–10] is the process of nuclear excitation by a resonant electron transition (NEET) from an excited electronic state to a lower-lying electronic state (Fig. 2). This is the inverse of internal conversion to bound states, evidence for which has been found recently in the internal conversion decay of highly ionized ions of ^{125}Te [11–14]. The possibility of excitation of ^{235m}U by an electron transition from a $6p$ to a $5d$ level was investigated in [8] and [9] where it was concluded that even at perfect resonance the NEET transition rate would be significantly smaller than the experimental rate reported in [3].

An alternative possibility is the process of nuclear excitation by electron capture (NEEC) [15,16] in which an electron is captured from the continuum into a bound orbital. This is the exact inverse of the well-known process of decay of nuclear states by internal conversion of bound electrons. The estimate for ^{235}U in [15] yielded a rate for NEEC that was 1000 times larger than the rate for NEET. Other nuclear excitation processes include inelastic electron scattering or photoexcitation by photon Bremsstrahlung generated from moving electrons. The driving effect of the electric field of a high power laser (with a photon energy of 5 eV) on the atomic electrons of ^{235}U was considered in [17]. In addition, a variant of NEET was treated in [18] where absorption of laser photons permits the energy mismatch between atomic and nuclear transitions to be reduced. The laser energy and intensity in the CO_2 laser experiments, however, appear to be well below those capable of giving significant nuclear excitation rates as a result of direct interactions between the laser and the atom-nucleus system. Nuclear excitation of ^{235m}U by simultaneous application of an x-ray and a laser beam using the inverse electron bridge process was considered in [19]. In this connection, it is noteworthy that the inverse electron bridge mechanism has been recently discussed in the context of the very low-energy (3.5 eV) isomeric state of ^{229m}Th [20–22]. Finally, the theory of excitation of collective nuclear rotational motion by an x-ray laser has been considered in [23].

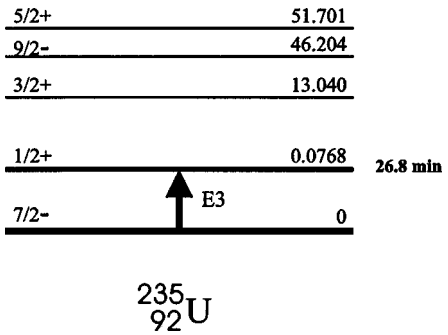

FIG. 1. Low-lying levels of ^{235}U.

TABLE I. Summary of experiments investigating the excitation of the isomeric state ^{235m}U in a plasma.

Experimental parameter	Izawa *et al.* [3]	Arutyunan *et al. A* [4]	Arutyunan *et al. B* [5]	Bounds and Dyer [6]
Method of plasma production	CO_2 laser	CO_2 laser	500 keV e^- beam 150 kA	CO_2 laser
Laser parameters	1 J, 100 ns	5 J, 200 ns		150 mJ, 35 μs + $\simeq 10^{15}$ W cm^{-2} 700 fs 5 eV
Plasma temp	$\simeq$100 eV		$\simeq$20 eV	
Plasma n_e (cm^{-3})	$\simeq 10^{19}$		3–30×10^{19}	
Experimental result	$\langle\sigma_N v_e\rangle$ $\simeq 10^{-20}$ cm^3 s^{-1}	$\sigma_N < 10^{-32}$ cm^2	σ_N $\simeq 5\times10^{-32}$ cm^2	$\lambda_{ex} < 6\times10^7$ s^{-1}
Nuclear excitation rate per ^{235}U (s^{-1}) (see Sec. II)	$\simeq 1$	$<10^{-5}$	$\simeq 3\times10^{-5}$	$<6\times10^7$

At the present moment, several experiments investigating laser-induced excitation of ^{235}U and other isotopes are planned or in progress. One object of this article is thus to consider the theory of nuclear excitation by the processes of NEET, NEEC, inelastic scattering, and photoexcitation which are likely to give the dominant contributions to the nuclear excitation rates, both with a view to understanding the existing experimental data and for guidance in the planning of future experiments. These nuclear excitation processes are considered in turn in Secs. III, IV, V, and VI. We use the case of excitation of ^{235}U as an example both because it appears to represent a particularly favorable case for experimental detection of nuclear excitation based on atom-nucleus coupling under plasma conditions and because the existing data lacks adequate theoretical explanation. In addition, before dealing with the theory of the different nuclear excitation mechanisms, we reconsider in Sec. II the nuclear excitation rates that are extracted from the experimental data, since the existing data appears to contain a number of inconsistencies.

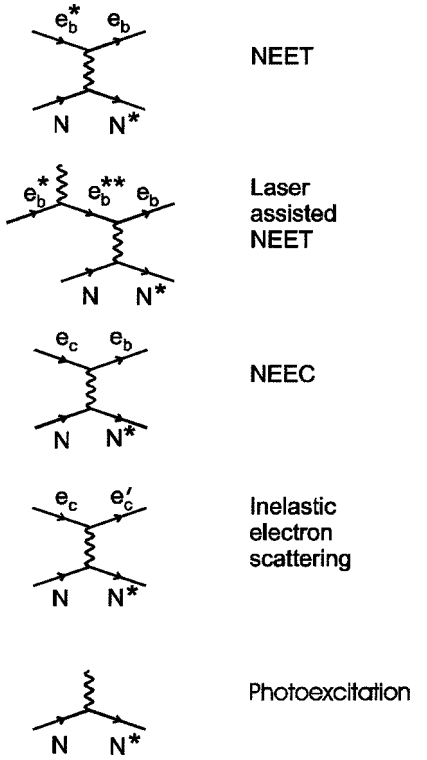

FIG. 2. Feynman diagrams for several possible nuclear excitation processes in plasmas. *N* indicates the nuclear ground state, *N** is a nuclear excited state. The label e indicates an electron state. The subscript b indicates a bound orbital and c a continuum orbital.

II. DISCUSSION OF EXPERIMENTAL DATA

A. Laser plasma experiment

The first experiment investigating nuclear excitation of ^{235}U in a plasma [3] used a TEA CO_2 laser and a natural uranium target. Uranium ions vaporized from the target were deflected in an electric field and collected on a plate. After 100 laser pulses (each of duration 100 ns) the plate was transferred to a detector which counted conversion electrons from the 26.8 minute decay of the 77 eV isomeric state. The nuclear excitation rate was extracted from the data on the basis of the following expression for the experimentally measured number, N_P, of ^{235m}U nuclei produced per pulse:

$$N_P = n_e n_U V \langle \sigma_N v_e \rangle \tau, \tag{1}$$

where n_e is the electron density, n_U is the density of ^{235}U nuclei, V is the plasma volume, v_e is the electron velocity in the plasma, and τ is the duration of the pulse. Under the experimental conditions it was estimated that $n_e = 10^{19}$ cm^{-3}, $V = 10^{-6}$ cm^3, and $\tau = 100$ ns. The ^{235}U density was obtained from $n_U = f_{235} N_U$ where f_{235} is the fraction of uranium present in the plasma present in the isotopic form ^{235}U ($=0.007$ for natural uranium) and N_U is the total uranium density for all isotopes in the plasma, which was assumed to be equal to the electron density. Using these estimates, the result for the cross section derived from Eq. (1) was $\langle \sigma_N v_e \rangle = 1.4\times10^{-20}$ cm^3 s^{-1}. In order to facilitate comparison between different experimental results it is useful to consider the excitation rate per nucleus of ^{235}U which will be denoted λ_N. In terms of the above parameters, λ_N

$=N_P/(n_U V\tau)$ yielding $\lambda_N \simeq 10^{-1}$ s^{-1}. It should be emphasized that this result is based on the assumption $N_U = n_e$. If the plasma, the temperature of which was estimated to be 100 eV in [5], is composed of multiply ionized uranium one would expect $N_U < n_e$. In Sec. III the charge-state distribution is found to peak around $q = 23+$. This would indicate that the uranium density should be reduced by a factor of approximately 23. In this case, the nuclear excitation rate per nucleus deduced from the data in [3] should be increased by the same factor, giving $\lambda_N \simeq 2$ s^{-1}.

B. Electron-beam experiment

In this experiment a 500 keV electron beam was incident on targets containing varying concentrations of ^{235}U up to 99.9% enriched. The target was heated by the electron beam, thus creating a plasma in which the estimated temperature was approximately 20 eV. Material blown off after plasma formation was collected on a nearby collector which was subsequently removed from the beam area and transferred to a detection system. The number of ^{235}U nuclei in this material was measured from the α-decay rate and the number of ^{235m}U nuclei was measured by counting internal conversion electrons from the deexcitation to the ground state. The experiment thus determined the ratio ξ equal to the number of ^{235m}U nuclei on collector divided by the total number of ^{235}U nuclei on the collector. The quoted excitation cross section σ_N was extracted using the relation

$$\xi \simeq n_e(T)\,\tau e^{-\Delta E/T} v_e \sigma_N , \tag{2}$$

where $n_e(T)$ is the electron density in the plasma, τ is the duration of an electron pulse, $\Delta E = 77$ eV is the excitation energy of the isomeric state, v_e is the velocity of a continuum electron with energy 77 eV and T is the plasma temperature. Inserting the quoted experimental result $\xi = 8.5 \times 10^{-13}$ (which was the maximum value of several different experimental results) yielded from Eq. (2), $\sigma_N = 10^{-32} - 10^{-31}$ cm^2. The cross section extracted in this way should be treated with caution. It should be emphasized that since the velocity which multiplies the cross section is that for a continuum electron of 77 eV, the value of σ_N derived from Eq. (2) refers, as does that derived from Eq. (1), to nuclear excitation occurring as a result of collisions between plasma electrons and atoms of ^{235}U. In the case of the electron-beam experiment, an alternative possibility exists: it is possible that the excitation is due to interactions of beam electrons with uranium nuclei, either directly, by inelastic electron scattering, or indirectly, by photoabsorption of Bremsstrahlung generated by electron impact on the uranium target. Theoretical estimates of the cross sections for these processes will be presented in the next section. We first derive a revised estimate of the cross section for nuclear excitation of ^{235}U nuclei by beam electrons, which is free from the assumption of transfer of energy from the plasma. If we denote the electron flux on the target by F_e and the number of atoms of ^{235}U per unit volume in the target n_U, then the number of isomeric nuclei produced per pulse is $\sigma_N F_e n_U \tau$. Thus $\xi = \sigma_N F_e \tau$. The electron flux is given simply by $F_e = I/eA$ with I being the electron-beam current, A is the area of the electron beam at the target, and e is the electron charge. From [5] $I = 150kA$ and the beam cross section was approximately 0.03 cm^2, corresponding to the reported beam diameter of 2 mm. These parameters yield an electron flux of 3×10^{25} cm^{-2} s^{-1} and a nuclear excitation cross section (for excitation by beam electrons) $\sigma_N \simeq 10^{-30}$ cm^2. Thus the cross section resulting from this analysis is between one and two orders of magnitude larger than that obtained from the analysis in [4], based on the assumption of nuclear excitation from the plasma. It should be emphasized that the latter cross section is given in terms of parameters that are quite different from those in Eq. (2) which is the basis of the result given in [4]. In particular, the present result is completely independent of the plasma temperature. We note also that the cross section extracted in [5] using Eq. (2) above should not be directly compared with the cross section extracted in [3] because the equation for the former cross section contains a factor of $e^{-77/20} = 0.021$ which is absent from the expression for the excitation rate in [3]. Omitting this factor from the cross section deduced from the data in [5] yields a value $\sigma_N = (2-20) \times 10^{-34}$ cm^2 for nuclear excitation by plasma electrons.

We can also use the experimental value for the ratio ξ to derive an estimate of the nuclear excitation rate per nucleus, λ_N. Since ξ is equal to the ratio of isomeric to ground-state nuclei in the plasma, we have $\xi = \lambda_N \tau$. This yields $\lambda_N = 3 \times 10^{-5}$ s^{-1}. The nuclear excitation rate thus deduced has the merit that it is independent of assumptions concerning the mechanism of excitation.

III. NUCLEAR EXCITATION BY ELECTRON TRANSITION (NEET)

NEET decay is the excitation of the nucleus with simultaneous deexcitation of the atomic electron system [7]. It is thus the inverse of the bound internal conversion process [11–13] in which a nucleus deexcites by excitation of a bound electron to a higher-lying bound orbital. If we consider a NEET transition from an initial atomic state denoted i to a final atomic state denoted f, the NEET process can only have non-negligible probability if the energy difference $E_i - E_f$ is close to the nuclear excitation energy $E_N^* - E_N$. As in the case of transitions by bound internal conversion (BIC) [11], the finite widths of the initial and final states allow transitions to occur when energy matching is not exact, that is when the energy mismatch, $\delta_{if} = E_i - E_f - (E_N^* - E_N)$, is nonzero. Experimental evidence for NEET has been presented in [24–28] where electron bombardment or photon irradiation of a target was used to generate atomic excited states that were supposed to subsequently undergo nuclear excitation by NEET. Doubts have, however, since been raised concerning the validity of these experiments and evidence has been presented indicating that at least a significant part of the measured nuclear excitation rate in the photon irradiation experiments can be attributed to nuclear excitation due to photoexcitation by Bremsstrahlung [29].

In principle, the excited electronic initial state required for NEET could be produced by a variety of methods. In the following we restrict the discussion to the case of a laser-produced plasma in which electron-ion or ion-ion collisions can produce excited electronic states with significant probabilities. If we consider nuclear excitation by NEET in a volume element $d\underline{r}$ at position $\underline{r}$ we can write the number of

nuclei excited per laser pulse as

$$N_{\mathrm{NEET}}=\int_{t=0}^{\infty}\int_{\underline{r}}\sum_{q}\sum_{if}P^{q,i}(n_e,T)\times\lambda_{\mathrm{NEET}}^{q,if}(n_e,T)\rho_U(n_e,T,\underline{r},t)d\underline{r}\,dt, \tag{3}$$

where $P^{q,i}(n_e,T)$ is the fraction of ions present in atomic state i of charge state q under plasma conditions described by an electron density n_e and temperature T, $\lambda_{\mathrm{NEET}}^{q,if}(n_e,T)$ is the rate (per nucleus of ^{235}U) for a NEET transition from the atomic state i to the atomic state f, and $\rho_U(n_e,T,\underline{r},t)$ is the density of ^{235}U nuclei at position $\underline{r}$ at time t. If we assume further that the plasma can be modeled with a single electron density, that the probability of a given charge state is position independent, and that the dominant excitation occurs during the laser pulse, then the rate, per nucleus, for nuclear excitation by NEET is given by

$$\lambda_{\mathrm{NEET}}=\sum_{q}\sum_{if}P^{q,i}(n_e,T)\lambda_{\mathrm{NEET}}^{q,if}\simeq N_{\mathrm{NEET}}/\tau, \tag{4}$$

where τ is the pulse duration. In general, the initial atomic state will decay predominantly by atomic transitions without nuclear excitation. Denoting the rate of these processes by $\lambda_A^{q,i}(n_e,T)$, we can write the total NEET rate as

$$\lambda_{\mathrm{NEET}}=\sum_{q}\sum_{if}P^{q,i}(n_e,T)\lambda_A^{q,i}(n_e,T)P_{\mathrm{NEET}}^{q,i}(n_e,T)=\sum_{q}\sum_{if}\overline{\lambda}_{\mathrm{NEET}}^{q,if}(\delta_{if}), \tag{5}$$

where $P_{\mathrm{NEET}}^{q,if}$ is the probability of a NEET transition from state i to state f and $\overline{\lambda}_{\mathrm{NEET}}^{q,if}(\delta_{if})$ is the effective NEET rate between states i and f.

The theory of NEET excitation has been considered by a number of authors [7–10,30–34]. The initial numerical results given in [7] are now understood to be overestimates owing to the use of an incorrect nucleus-electron interaction potential. In the following, we assume that the initial and final atomic state widths are dominated by the atomic level widths, Γ_i and Γ_f. For the case that the condition $|\delta_{if}|\gg|V_{if}|$ is satisfied, the NEET probability can be written in the form [8,9]

$$P_{\mathrm{NEET}}^{q,i}=\left(1+\frac{\Gamma_f}{\Gamma_i}\right)\frac{V_{if}^2}{\delta_{if}^2+\frac{1}{4}(\Gamma_f+\Gamma_i)^2}, \tag{6}$$

where V_{if} is the matrix element between the initial and final atom-nucleus states.

In the calculations described below, the atomic states are described in the multiconfiguration Dirac-Fock approximation so that the initial- and final-state wave functions, Ψ_i,Ψ_f, are given by

$$\Psi_i(J_i,M_i)=\sum_{r}c_{ir}\psi_r(J_i,M_i), \tag{7}$$

$$\Psi_f(J_f,M_f)=\sum_{s}c_{fs}\psi_s(J_f,M_f), \tag{8}$$

where $\psi_r(J_i,M_i)$ and $\psi_s(J_f,M_f)$ are configuration state functions where J_i and J_f are the total angular momenta of the initial and final atomic states and M_i and M_f are their z components. The theory developed in [8,9] treated the case of initial and final states consisting of a single electronic configuration in which coupling effects of the active electron with the other atomic electrons were ignored. Extending the results of [8,9] to the multiconfigurational case, yields the following result for the squared matrix element V_{if}^2:

$$V_{if}^2=4\pi\alpha\left(\sum_{r}\sum_{s}c_{ir}c_{fs}d_{j_i,j_f}^{L}(r,s)\right)^2\times\frac{(2j_i+1)}{(2J_i+1)}\frac{\omega_N^{2(L+1)}}{[(2L+1)!!]^2}\left(j_i\frac{1}{2}L0\middle|j_f\frac{1}{2}\right)^2\times|M_L(\omega_N)|^2B(EL), \tag{9}$$

where α is the fine-structure constant, $d_{j_i,j_f}^{L}(r,s)$ is a coefficient arising in the calculation of one particle tensor operators of rank L between orbitals with total angular momenta j_i and j_f in configuration states r and s [35], $B(EL)$ is the nuclear electromagnetic transition moment from the ground to the excited nuclear state, $\hbar\omega_N=E_N^*-E_N$ and the quantity $M_L(\omega_N)$ is the electronic matrix element, which for an electric multipole transition, is given by

$$M_L(\omega_N)=\int[P_{n\kappa}(r)P_{n'\kappa'}(r)+Q_{n\kappa}(r)Q_{n'\kappa'}(r)]h_L(\omega_N r)-\frac{h_{L-1}(\omega_N)}{L}[(\kappa-\kappa'-L)P_{n\kappa}(r)Q_{n'\kappa'}(r)+(\kappa-\kappa'+L)Q_{n\kappa}(r)P_{n'\kappa'}(r)]dr, \tag{10}$$

where $P_{n\kappa}(r)/r$ and $Q_{n\kappa}(r)/r$ are the large and small components of the wave function for the electronic subshell $n\kappa$. The quantity $h_L(\omega_N r)$ is the Hankel function of order L.

In [8,9] it was suggested that the most important contributions to the NEET rate would arise from the three atomic transitions: $6p_{1/2}\rightarrow5d_{5/2}$, $6p_{3/2}\rightarrow5d_{3/2}$, and $6p_{3/2}\rightarrow5d_{5/2}$. In order to investigate this in more detail, we have calculated NEET transition energies and matrix elements for these three transitions in ions ranging from $q=7+$ (described by the manifold [Xe] $6s^24f^{14}5d^96p^6$) to $q=12+$ (described by the manifold [Xe] $6s^24f^{14}5d^96p^1$). On the basis of the discussion of charge-state probabilities given below, these ionic states are expected to be dominant in plasmas with $T\simeq20$ eV. The $6p_{1/2}\rightarrow5d_{5/2}$ transition satisfies the energy matching condition most closely, giving rise to one or more resonances lying within a few eV of the nuclear transition energy in each charge state. Multiple resonances arise from the coupling of spectator electrons with the active electron undergoing the transition. This effect is shown for the case of U^{10+} in Fig. 3 for NEET transitions between states described by the manifolds [Xe] $6s^24f^{14}5d^96p^3$ and [Xe] $6s^24f^{14}5d^{10}6p^2$. Coupling between the $5d$ and $6p$ electrons, and between the open shell $6p$ electrons, splits the electronic

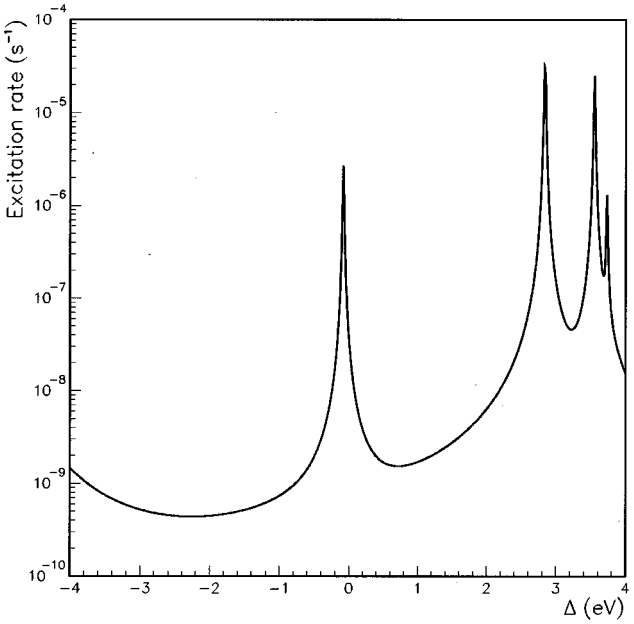

FIG. 3. Nuclear excitation probability as a function of the uncertainty Δ_{if} in the transition energy for NEET resonances arising from the $6p_{1/2}\rightarrow 5d_{5/2}$ transition in the ion U^{10+} $[Xe]6s^2 4f^{14}5d^9 6p^3$ for a plasma at 20 eV.

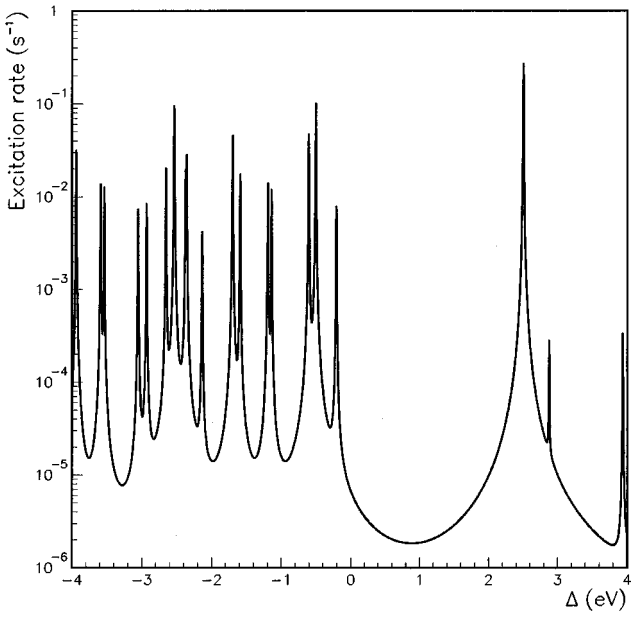

FIG. 4. Nuclear excitation probability as a function of the uncertainty Δ_{if} in the transition energy for NEET resonances arising from the $6d_{5/2}\rightarrow 6p_{1/2}$ transition in the ion U^{22+} $[Xe]4f^{14}5d^1 6d^1$ for a plasma at 100 eV.

transition $6p_{1/2}\rightarrow 5d_{5/2}$ into several branches, four of which lie in the interval with $|\delta_{if}|<4$ eV. Each peak, the intensities of which are discussed below, describes a resonance with an energy mismatch δ_{if} equal to the Δ value at the center of the peak.

In general for a given electronic transition between two subshells, the matrix elements, V_{if}^2, depend on the mixing coefficients and subshell occupation numbers of the electron configurations in the initial and final states. For those transitions which occur between atomic states that are dominated by a single configuration having the maximum occupancy of the $6p_{1/2}$ subshell, the matrix elements in the ions with $q\simeq 10+$ are such that $V_{if}^2=(2.0-2.5)\times 10^{-18}$ eV^2. These values are slightly smaller than the result $V_{if}^2=5\times 10^{-18}$ eV^2 reported in [9] but four orders of magnitude larger than the result $V_{if}^2=2.4\times 10^{-23}$ eV^2 reported in [18]. The difference between the present result and the result of [9] arises principally from the neglect in [9] of Pauli blocking by the $5d$ electrons present in the initial state. The difference between the present result and that of [18] arises principally from the different approximations used for the electron wave functions. In [18] a nonrelativistic hydrogenic approximation was employed with an effective nuclear charge, $Z_{\rm eff}$ chosen to reproduce the correct electron binding energy. This approach underestimates the NEET matrix elements which are dominated by the small-r behavior of h_L for which

$$h_L(\omega_N r)\simeq\frac{(2L-1)!!}{(\omega_N r)^{L+1}}. \tag{11}$$

Thus for an $E3$ transition $h_L\sim r^{-4}$, in contrast to the energy operator which weights the matrix elements to larger radial distances. This has the consequence that the effective nuclear charges $Z_{\rm eff}$ appropriate for calculating electronic matrix elements that determine internal conversion, or NEET, involving $5d$ or $6p$ orbitals of uranium, are in the region of $Z_{\rm eff}\simeq 50$ in contrast with values of $Z_{\rm eff}\simeq 10-15$ that optimize the energy. We have verified that a recalculation of the NEET matrix element using hydrogenic wave functions with $Z_{\rm eff}\simeq 50$ yields values for V_{if}^2 that are in reasonable agreement (within 50%) with the values calculated using Dirac-Fock wave functions. Decreasing $Z_{\rm eff}$ to $\simeq 10-15$ reduces V_{if}^2 by four to five orders of magnitude. This thus explains the very small values for V_{if}^2 estimated in [18] for ^{235}U.

As discussed above, the $6p_{1/2}\rightarrow 5d_{5/2}$ transition is nearly resonant in ions with $q\simeq 10+$. As the ionic charge is increased, the probability of a $6p$ electron being present in the initial state decreases and the energy matching becomes poorer, with the result that the transition moves out of resonance. At the same time, other transitions that have $\delta_{if}<0$ in low charge states, move closer to resonance in higher charge states. Of particular interest is the transition $6d_{5/2}\rightarrow 6p_{1/2}$ which lies close to resonance in ions with $q\simeq 23+$. Thus, in the initial state ion U^{23+} $[Xe]4f^{14}6d^1$ the Dirac-Fock result for the transition energy is 77.3 eV corresponding to an energy mismatch of 0.5 eV. The atomic configuration in this state of U^{23+} is particularly simple since, apart from the single $6d$ electron, the atom has a closed shell configuration. When the ion has a more complex open-shell configuration, interactions between the active electron and electrons in open shells can again split the transition into a number of branches. An example of this effect is shown in Fig. 4 for the case of the initial state ion $q=22+$ described by the manifold $[Xe]4f^{14}\,5d^1 6d^1$. The coupling of the $5d$ electron with the $6d_{5/2}$ or $6p_{1/2}$ electron splits the $6d_{5/2}\rightarrow 6p_{1/2}$ transition into 20 branches lying within 4 eV of resonance. The dominant transitions have electronic matrix elements correspond-

ing to values of $V_{if}^2 \simeq 2\times 10^{-18}$ eV^2, of the same order of magnitude as those for the $6p_{1/2} \rightarrow 5d_{5/2}$ transition in ions with $q \simeq 10+$. The above estimates of the matrix elements imply that the condition $|\delta_{if}| \gtrsim |V_{if}|$ is satisfied as long as $\delta_{if} \gtrsim 10^{-8}$ eV.

In order to obtain numerical estimates of the NEET rate from Eqs. (5) and (6), one needs to know, in addition to the atomic energy levels discussed above, the atomic level widths. In the absence of a laser field, the initial electron hole state can decay by both radiative and Auger decay. For example, for the case of an isolated uranium atom containing a $5d$ hole, the transition rate for filling of the hole by an $E1$ radiative transition of an electron in one of the $6p$ orbitals is of the order of 10^{10} s^{-1}, corresponding to a natural width for the initial state of the order of 10^{-5} eV. Under plasma conditions, the level widths are dominated by Stark broadening. An estimate of the effect of electron broadening contribution to the Stark width of an electronic transition in an ion, charge q, in a plasma is given by twice the electron-ion collision frequency [36]

$$\Gamma \simeq 5\times 10^{-21} n_e q T_e^{-1.5} [23 - \ln(n_e^{1/2} q T_e^{-3/2})], \qquad (12)$$

with the electron density n_e in cm^{-3} and the temperature T_e in eV. For the dominant charge states in the temperature range 20–100 eV the above relation gives transition widths of the order of 5–20 meV.

The absolute nuclear excitation rates are obtained by multiplying the rates $\lambda_{\mathrm{NEET}}^{q,if}$ for a given atomic transition by the probabilities, $P^{q,i}(n_e,T)$, where the given hole states are present in the plasma. In order to determine the approximate population density in different charge states, we use the collisional-radiative model of the plasma [37]. In this model, the plasma is assumed to be homogeneous and the energy distributions of the electrons and ions are described by a Maxwellian distribution with a single temperature T. Under stationary state conditions the ratio between populations of successive charge states is given in terms of the rate coefficients for the processes of collisional ionization, radiative recombination and three-body recombination. The ionization energies for different charge states of uranium up to 40+ have been estimated here from the atomic binding energies using the relativistic atomic structure package GRASP [38]. The results are shown in Fig. 5. For configurations with closed f shells all configurations belonging to a given manifold were used. For configurations containing open f shells it was necessary to limit the number of configurations used in the calculation. Thus a single j-j coupled configuration was taken for the open f-shell electrons and this was then coupled onto all possible configurations for the remaining electrons.

Using the Dirac-Fock values for the binding energies, the populations $P^q(n_e,T)$ of charge states q in a plasma with electron density, $n_e = 10^{19}$ cm^{-3}, at plasma temperatures $T = 5$, 20, and 100 eV, calculated on the basis of the collisional-radiative model are shown in Fig. 6. The dominant charge state in a uranium plasma at 100 eV is found to be $q = 23+$, in a plasma at 20 eV it is $q = 10+$ and in a plasma at 5 eV it is $q = 6+$. In all cases the ion population is strongly peaked around the dominant charge state so that effectively only a few charge states are significantly populated. Using values of $P^q(n_e,T)$ for the ground-state populations, we estimate the populations of excited states that may undergo NEET transitions on the basis of a Boltzmann distribution. Formation of the $5d$ hole states in ions with $q \simeq 10+$ requires an excitation energy, $E_{\mathrm{ex}} \simeq 77$ eV, while formation of excited $6d$ states in ions with $q \simeq 23+$ requires $E_{\mathrm{ex}} \simeq 240$ eV.

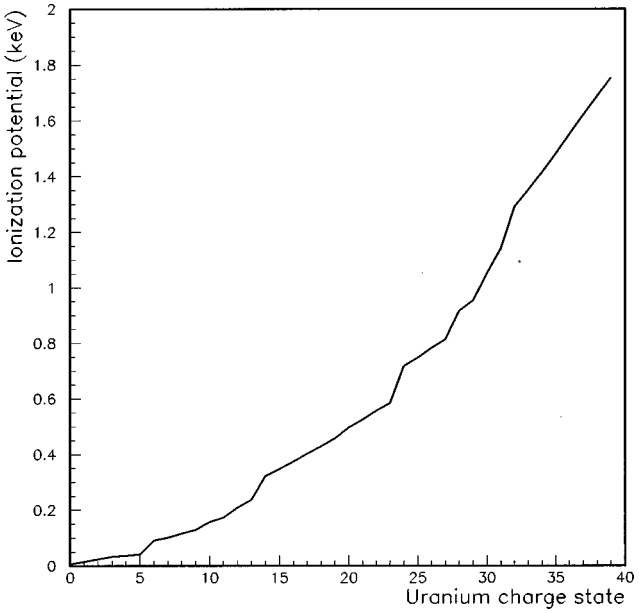

FIG. 5. Ionization energies (in eV) for uranium as a function of charge state.

The calculated resonance energies are subject to an uncertainty Δ_{if}, arising both from an uncertainty in the nuclear transition energy (0.5 eV) as well as an uncertainty in the atomic transition energy. The latter arises both from the neglect of electron correlation in the Dirac-Fock approximation itself as well as from the shift of the atomic electron energies

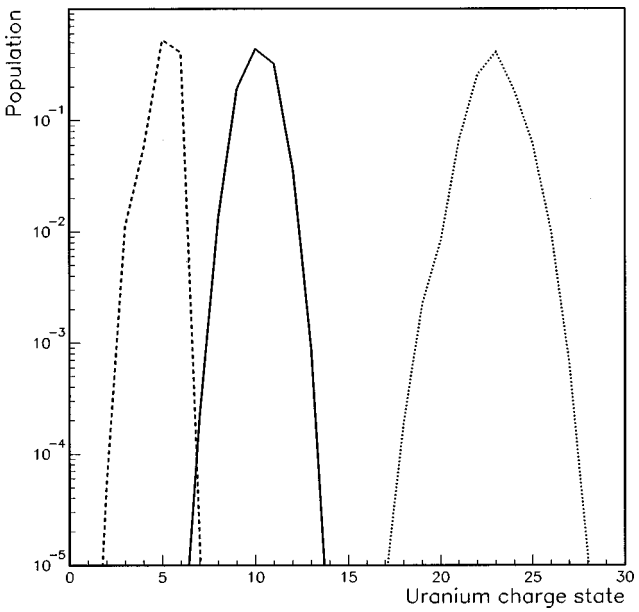

FIG. 6. Populations of different ionic states of uranium in a plasma with mean temperature 5 eV (long dashes), 20 eV (solid line), and 100 eV (short dashes) based on the collisional-radiative model.

due to interactions with the electrons and ions in the plasma. Comparison of GRASP results with ionization potentials for $5d$ electrons in high Z atoms indicates that the error due to neglect of electron correlation is approximately 2 eV. From the estimates of the level widths given above, we expect that the energy shifts will be less than 0.1 eV. Thus we have $\delta_{if}=\delta_{if}^{\mathrm{DF}}\pm\Delta_{if}$ where $\delta_{if}^{\mathrm{DF}}$ are the values of the energy mismatch based on the atomic transition energies calculated above in the Dirac-Fock approximation, and Δ_{if} is the error in the resonance energy. On the basis of the above discussion we expect $|\Delta_{if}|\lesssim 3$ eV. Figures 3 and 4 show the NEET rates, $\Sigma_f\overline{\lambda}_{\mathrm{NEET}}^{q,if}(\delta_{if}^{\mathrm{DF}}+\Delta_{if})$, estimated using Eqs. (5), (6), and (9) as a function of the parameter Δ_{if} for values of $|\Delta_{if}|<4$ eV for a particular initial state described by a single set of orbital occupation numbers. Contributions from overlapping resonances in the many different highly excited states populated in the plasma lead to broadening of the NEET spectrum. The variation in the NEET rates with Δ_{if} can then be used to derive lower and upper bounds on λ_{NEET}. Thus at 100 eV we obtain $10^{-6}\ \mathrm{s}^{-1}<\lambda_{\mathrm{NEET}}<1\ \mathrm{s}^{-1}$ and at 20 eV $10^{-9}\ \mathrm{s}^{-1}<\lambda_{\mathrm{NEET}}<10^{-4}\ \mathrm{s}^{-1}$. The rates at 20 eV are lower than those at 100 eV essentially due to the fact that the dominant atomic states in which resonance is approached at 20 eV are present with lower probabilities $P^{q,i}$ than is the case at 100 eV. These estimates clearly demonstrate the sensitivity of the NEET rates to the charge-state distribution and the plasma temperature. The sensitivity of the NEET rate to plasma conditions could be one factor responsible for the difference between the experimental rates. This conclusion is also indicated by calculations of NEET rates [39] averaged over the ± 0.5 eV uncertainty in the nuclear excitation energy, employing charge-state distributions based on a model of local thermodynamic equilibrium.

As far as future experiments investigating NEET in ^{235}U are concerned, the above results indicate that the NEET rate can be maximized in plasmas with temperatures of between 10 and 150 eV by maximizing the population of ions with $q\simeq 23+$.

IV. NUCLEAR EXCITATION BY ELECTRON CAPTURE (NEEC)

NEEC (nuclear excitation by electron capture) is the excitation of the nucleus by capture of a continuum electron into a bound orbital. This process is formally the inverse of the usual internal conversion process in which a nucleus deexcites by ejection of an electron from a bound orbital into the continuum. The electron orbitals that may contribute significantly to NEEC capture in a particular ion depend on the atomic structure of this ion and are thus not necessarily the same as those that participate in the internal conversion decay process of neutral or nearly neutral atoms.

If we denote the energy of the captured continuum electron by E and the binding energy of the bound electron after capture by E_b then, given an initial state containing a distribution of continuum electron energies, the condition $E=E_N-E_b$ can be satisfied exactly for some value of the continuum electron energy, provided $E_N>E_b$. Thus in general, a large number of bound orbitals can participate in the NEEC process. In addition, in principle, the NEEC process does not require the initial bound electronic state to be excited, provided there is a source of continuum electrons. Thus, for example, capture could occur onto a ground-state uranium ion without the requirement for a $5d$ or $6p$ hole. On the other hand, NEEC matrix elements for highly excited orbitals tend to be less than those for lower-lying orbitals so that one might expect a reduction in the probability for continuum capture with increasing principal quantum number of the orbital into which capture occurs.

A crude estimate of the probability of NEEC in a plasma was presented in [15] where the rate for NEEC was found to be of the order of 1000 times larger than the rate for NEET decay from a bound initial state. However this estimate was based on a number of approximations of dubious validity, including a nuclear excitation cross section that was independent of nuclear parameters. More recently, NEEC excitation has also been considered for several isomers [16] by a scaling procedure applied to results for the process of resonant transfer excitation in which an electron in a solid target is captured into a bound orbital of a moving projectile ion. In this latter case the NEEC cross section was given in terms of the product of an Auger decay cross section and a ratio of quantities pertaining to the Auger decay rate and the internal conversion decay rate. The degree of approximation introduced by this scaling procedure is not clear and no numerical results were given for ^{235}U excitation. In the following the theory of the NEEC process is reconsidered with an explicit treatment of the electron-nucleus interaction.

We consider an initial state i in an ion of charge q. The total rate of NEEC transitions is given by

$$\lambda_{\mathrm{NEEC}}=\sum_q\sum_i\sum_{n\kappa}P^{q,i}(n_e,T)\lambda_{\mathrm{NEEC}}^{q,i,n\kappa}, \tag{13}$$

where the rate for NEEC capture to subshell $n\kappa$ is given by

$$\lambda_{\mathrm{NEEC}}^{q,i,n\kappa}=\int_{E=0}^{\infty}\sigma_{\mathrm{NEEC}}^{q,i,n\kappa}(E)F_e(E)dE, \tag{14}$$

where $\sigma_{\mathrm{NEEC}}^{q,i,n\kappa}(E)$ is the NEEC cross section at the energy E and $F_e(E)$ is the electron flux at this energy. Treating the NEEC capture as a resonance in the elastic scattering of electrons off the nucleus, the cross section, in lowest order, for formation of a resonance state containing the isomeric nuclear state is given by

$$\sigma_{\mathrm{NEEC}}^{q,i,n\kappa}(E)=\frac{\pi}{2k^2}S\frac{\Gamma_N^{q,i,n\kappa}\Gamma_t^{q,i}}{(E_r-E)^2+(\Gamma_t^{q,i})^2/4}, \tag{15}$$

where k is the wave number of the continuum electron of energy E, $\Gamma_N^{q,i,n\kappa}$ is the width of the resonance state for breakup to the initial scattering state, $\Gamma_t^{q,i}$ is the total width, and E_r the resonance energy. The factor S is a function of the nuclear spins, j_n and j_n' in the ground and excited states, the total angular momentum, j of the captured electron and the total angular momentum, j', of the continuum orbit from which capture occurs. S is given by

$$S=\frac{(2j_n'+1)(2j'+1)}{2(2j_n+1)(2j+1)}. \tag{16}$$

For a narrow transition, the cross section may be approximated by a δ function

$$\sigma_{\mathrm{NEEC}}^{q,i,n\kappa}(E)=\frac{2\pi^2}{k^2}S\Gamma_N^{q,i,n\kappa}(E)\,\delta(E_r-E). \tag{17}$$

The width $\Gamma_N^{q,i,n\kappa}$ is given by

$$\Gamma_N^{q,i,n\kappa}(E)=2\pi\int |\langle\psi_f|\hat{V}|\psi_i\rangle|^2\delta(E-E_N-E_{n\kappa})dk. \tag{18}$$

Using the result for the internal conversion matrix element in [40] gives the following expression for the NEEC rate:

$$\lambda_{\mathrm{NEEC}}^{q,i,n\kappa}=\sum_{n\kappa}\frac{16\pi^4}{k_r^2}S\alpha\omega_N^{2L+2}\times\frac{1}{[(2L+1)!!]^2}(j_c\ 1/2\ \ L0|j_b1/2)^2\times B(EL)|R_{n\kappa}^{XL}(E_r)|^2F_e(E_r), \tag{19}$$

where k_r and E_r are the wave number and energy corresponding to the resonance condition and $F_e(E_r)$ is the electron flux at the resonance energy. The quantities j_c and j_b appearing in the Clebsch-Gordon coefficient are the total angular momenta of the continuum and bound electron, respectively. The quantity $R_{n\kappa}^{XL}(E')$ is the matrix element for decay of the resonance state by internal conversion of a bound-state electron defined by the quantum numbers to a continuum state orbital of energy E'. If penetration effects are ignored, the electric multipole matrix element $R_{n\kappa}^{EL}$ is given by

$$R_{n\kappa}^{EL}(E')=\int[P_{n\kappa}(r)P_{E'\kappa'}(r)+Q_{n\kappa}(r)Q_{E'\kappa'}(r)]h_L(\omega_N r)-\frac{h_{L-1}(\omega_N r)}{L}[(\kappa-\kappa'-L)P_{n\kappa}(r)Q_{E'\kappa'}(r)+(\kappa-\kappa'+L)Q_{n\kappa}(r)P_{E'\kappa'}(r)]dr, \tag{20}$$

where $P_{E'\kappa'}(r)/r$ and $Q_{E'\kappa'}(r)/r$ are the large and small components of the wave function for the continuum electron normalized on the energy scale. For completeness the expression for the magnetic multipole matrix element is $R_{n\kappa}^{ML}$, given by

$$R_{n\kappa}^{ML}(E')=\frac{1}{2}\int[P_{n\kappa}(r)Q_{E'\kappa'}(r)+Q_{n\kappa}(r)P_{E'\kappa'}(r)]h_L(\omega_N r)dr, \tag{21}$$

where $P_{n\kappa}(r)/r$ and $P_{E'\kappa'}(r)/r$ are the large components of the wave function for the bound and continuum electron, respectively, and $Q_{n\kappa}(r)/r$ and $Q_{E'\kappa'}(r)/r$ are the corresponding small components of the electron wave function.

In the numerical estimates of NEEC rates presented below, a Maxwellian distribution, $P(E,T)$, of continuum electron energies has been assumed given by

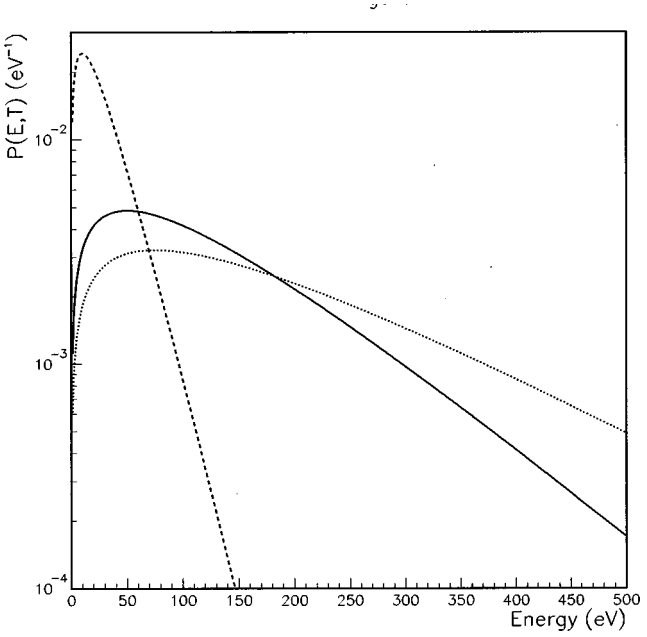

FIG. 7. Maxwell-Boltzmann distributions of plasma electron energies for a plasma with $T=20$ eV (long dashes), $T=100$ eV (solid line), and $T=150$ eV (dotted line).

$$P(E,T)=\frac{4\pi\sqrt{2E}}{(2\pi kT)^{3/2}}e^{-E/kT}. \tag{22}$$

This distribution is plotted in Fig. 7 for plasma temperatures, T, of 20, 100, and 150 eV. The electronic matrix elements are computed in a relativistic hydrogenic approximation. Screening effects on the electronic matrix elements are important and some care has to be taken in order to choose the effective nuclear charges in an appropriate way. The basic procedure adopted here is to select the nuclear charge for the hydrogenic functions so as to reproduce an appropriate expectation value for bound orbitals that can be calculated simply using Dirac-Fock wave functions. In order to do this, we note that the small r behavior of the Hankel function, $h_L(\omega r)$, that appears in the transition-matrix element is given by Eq. (11). Numerical evaluation shows that this limiting function provides a reasonable estimate of the Hankel function in the regions that contribute significantly to the integral in the matrix element. For the excitation of ^{235}U, we thus choose the effective nuclear charge for $j=l+1/2$ bound orbitals so as to reproduce expectation values of r^{-4} for these orbitals. It is convenient to use the same effective nuclear charge to describe the $j=l-1/2$ orbital with the same value of the principal quantum number. We have verified that a calculation of the internal conversion coefficient of uranium for the dominant $6p_{1/2}$, $6p_{3/2}$, and $6d_{3/2}$ orbitals using relativistic hydrogenic wave functions with values of $Z_{\mathrm{eff}}\simeq 50$ obtained in this way agrees to within a factor of 4 with literature values for the internal conversion coefficient reported in [40], calculated with Dirac-Fock bound and continuum electron wave functions.

In principle, the number of high-lying orbitals satisfying the energy condition $E_b<E_N$ eV can be very large. However, we note that, for the case of the $E3$ transition of ^{235}U, capture into p and d orbitals dominates since this allows the

TABLE II. Rates $\lambda_{\mathrm{NEEC}}^{q,i,n\kappa}$ for nuclear excitation by electron capture (NEEC) to the isomeric state of ^{235}U for capture in subshell $n\kappa$ of U^{6+} and U^{10+} ions in a plasma at 20 eV with $n_e=10^{19}$ cm^{-3}. E_r is the energy of the continuum electron for resonant capture.

Subshell	U^{6+}		U^{10+}	
nl_j	E_r (eV)	$\lambda_{\mathrm{NEEC}}^{6+,n\kappa}$ (10^{-12} s^{-1})	E_r (eV)	$\lambda_{\mathrm{NEEC}}^{10+,n\kappa}$ (10^{-12} s^{-1})
$6d_{3/2}$	26.4	1.2	<0	0
$6d_{5/2}$	22.4	3.8	<0	0
$7p_{1/2}$	38.8	1.0	9.7	11
$7p_{3/2}$	41.4	3.0	4.8	46
$7d_{3/2}$	49.9	0.07	17.4	1
$7d_{5/2}$	50.3	0.3	18.5	4
$8p_{1/2}$	54.0	0.2	27.2	2
$8p_{3/2}$	55.2	0.6	29.7	6
Total		10		70

bound and continuum electrons to share the angular momentum of the transition and maximizes the electronic matrix elements. In order to investigate the basic characteristics of NEEC, we consider capture in three ionic states: U^{6+} [Rn], U^{10+} [Xe]$6s^24f^{14}5d^{10}$, and U^{24+} [Xe]$4f^{14}$. Table II shows excitation rates per nucleus $\lambda_{\mathrm{NEEC}}^{q,i,n\kappa}$ for capture into p and d orbitals of U^{6+} and U^{10+} in a plasma of temperature 20 eV in which the electron density is 10^{19} cm^{-3}. Similarly Table III shows results for U^{24+} in a 100 eV plasma for $n_e=10^{19}$ cm^{-3}. The excitation rates have been summed over the dominant continuum orbitals that can contribute to capture into a given bound orbital, taking into account the restrictions imposed by the Clebsch-Gordon coefficient and by

TABLE III. Rates $\lambda_{\mathrm{NEEC}}^{q,i,n\kappa}$ for nuclear excitation by electron capture (NEEC) to the isomeric state of ^{235}U capture in subshell $n\kappa$ of U^{24+} ions in a plasma at 100 eV with $n_e=10^{19}$ cm^{-3}. E_r is the energy of the continuum electron for resonant capture.

Subshell nl_j	E_r (eV)	$\lambda_{\mathrm{NEEC}}^{24+n\kappa}$ (10^{-12} s^{-1})
$12p_{3/2}$	5.8	2.9
$13p_{3/2}$	17.6	1.9
$14p_{3/2}$	26.7	1.3
$15p_{3/2}$	33.5	1.0
$16p_{3/2}$	39.2	0.7
$17p_{3/2}$	44.2	0.6
$18p_{3/2}$	48.0	0.5
$12p_{1/2}$	4.0	0.9
$13p_{1/2}$	16.2	0.6
$14p_{1/2}$	25.6	0.4
$15p_{1/2}$	32.6	0.3
$16p_{1/2}$	38.5	0.2
$17p_{1/2}$	43.6	0.2
$18p_{1/2}$	47.6	0.1
$12d_{3/2}$	9.6	0.2
$12d_{5/2}$	10.0	0.7
Total		12

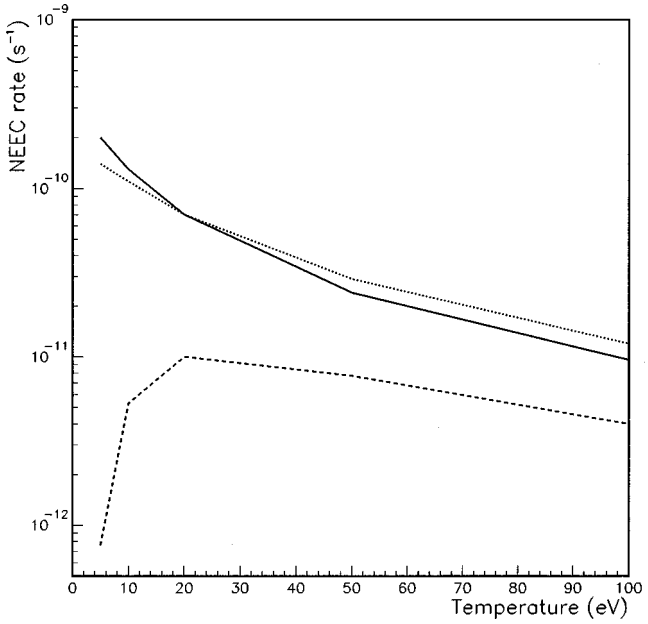

FIG. 8. The NEEC excitation rate as a function of temperature for U^{6+} (long dashes), U^{10+} (solid line), and U^{24+} (short dashes) ions. In each case the plasma density is $n_e=10^{19}$ cm^{-3}.

the symmetry requirement that l_b+l_c+L must be even for an electric multipole transition. The temperature dependence of the NEEC rates, $\Sigma_{n\kappa}\lambda_{\mathrm{NEEC}}^{q,i}$, summed over the orbitals $n\kappa$ shown in Tables II and III is shown in Fig. 8. The experimental nuclear excitation rate is the product of the above NEEC rate and the population of the given ion in which capture occurs. If the atomic state populations, $P^{q,i}(n_e,T)$ of the most probable charge states are of the order of 0.1, as indicated by the discussion in Sec. II A, then the above calculations, together with Eq. (13) indicate that nuclear excitation rates due to NEEC are of the order of 10^{-11} s^{-1} in plasmas with $n_e\simeq10^{19}$ cm^{-3} at temperatures in the range 20–100 eV. Nuclear excitation by NEEC thus appears to be significantly less probable than excitation by the NEET process discussed above. Results for NEEC excitation of other nuclei will be presented elsewhere [41].

V. INELASTIC ELECTRON SCATTERING

Electrons that have energies greater than the nuclear excitation energy may cause nuclear excitation in collisions by inelastic scattering [42–46]. If the electron energies are sufficiently high, as for example is the case in the electron-beam experiment of [5], inelastic scattering may also lead to excitation of high-lying excited nuclear states that subsequently decay to the isomeric state. The effective cross section for formation of the isomeric state can thus be written $\sigma_{\mathrm{eff}}^{e}=\Sigma_n\sigma_n^eY_n$ where σ_n is the cross section for formation of the state, n, and Y_n is the probability that the decay of this state eventually populates the 77 eV isomeric level.

A discussion of the cross sections for inelastic scattering of ^{235}U by 500 keV electrons is given in [47]. The dominant cross sections were found to be of order $10^{-33}-10^{-32}$ cm^2 for excitation of levels of the 5/2[622] and 5/2[333] bands for which the bandheads lie at 129 and 333 keV, respectively. Combining these results with an electron flux of 3

TABLE IV. Parameters describing the resonant photoexcitation of ^{235}U by 500 keV electrons.

Excited nuclear state n	Energy (keV)	Y_n (cm)	λ_n	Γ_n^γ (eV)	$\sigma_n^\gamma(E_\gamma=E_N)$ (cm^2 eV)	σ_n^p (cm^2)
$\frac{7}{2}+(1/2[631])$	0.077	1.0	1.6×10^{-6}	1.6×10^{-39}	1.1×10^{-50}	9×10^{-55}
$\frac{3}{2}+(1/2[631])$	13.0	1.0	9.5×10^{-9}	4.0×10^{-18}	2.7×10^{-33}	1×10^{-39}
$\frac{5}{2}+(1/2[631])$	51.7	1.0	2.4×10^{-9}	1.3×10^{-12}	5.3×10^{-29}	6×10^{-36}
$\frac{5}{2}+(5/2[622])$	129.3	0.15	9.6×10^{-10}	6.5×10^{-9}	4.5×10^{-26}	2×10^{-33}
$\frac{5}{2}+(5/2[633])$	332.8	0.17–0.22	3.7×10^{-10}	1.1×10^{-7}	1.2×10^{-25}	1×10^{-33}

$\times10^{25}$ cm^{-2} s^{-1} yields nuclear excitation rates of order $3\times10^{-8}-3\times10^{-7}$ s^{-1}. In view of the significant difference between this rate and the experimental rate of 3×10^{-5} s^{-1} deduced from the data of [5], an explanation of the data in terms of electron scattering alone appears unsatisfactory.

Excitation of the isomeric state by inelastic scattering of plasma electrons is, in principle, possible. However, an estimate of the rate for excitation of the isomeric state, for a plasma of temperature 100 eV using the Born approximation, yields $\lambda_n\approx10^{-16}$ s^{-1}, negligible in comparison with the experimental excitation rates. Production of the isomeric state by inelastic scattering to higher-lying nuclear states is even less likely due to the low probability that an electron has the necessary kinetic energy to excite a nuclear state.

VI. PHOTOEXCITATION

Nuclear absorption of Bremsstrahlung produced by charged particle motion in the plasma is an additional mechanism that might populate isomeric states, either by a direct photoexcitation of the isomeric level or by photoexcitation to a higher level followed by decay to the isomeric level. The cross section $\sigma_n^\gamma(E_\gamma)$ for resonant photoexcitation to a nuclear level n (with excitation energy E_N) by photons of energy E_γ, is given by [48]

$$\sigma_n^\gamma(E_\gamma)=\frac{\pi}{2}g_n\lambda_n^2\frac{\Gamma_n^\gamma\Gamma_t}{(E_\gamma-E_N)^2+\Gamma_t^2/4}, \tag{23}$$

where λ_n is the transition wavelength, Γ_n^γ is the γ decay width of the excited state, Γ_t is the total width of the excited state, and g_n is a statistical factor equal to $(2j_n'+1)/(2j_n+1)$ with j_n and j_n' the nuclear spins in the ground and isomeric nuclear states, respectively. For a narrow resonance, the Breit-Wigner form may be approximated by a δ function giving $\sigma_n^\gamma(E_\gamma)=\pi^2g_n\lambda_n^2\Gamma_n^p\delta(E_\gamma-E_N)$.

The number of Bremsstrahlung photons emitted per second with energies between E_γ and $E_\gamma+dE_\gamma$ produced by electrons of energy E is

$$R_\gamma(E_\gamma)=VN_U\frac{d\sigma_B(E)}{dE_\gamma}dE_\gamma F_e(E)dE, \tag{24}$$

where V is the volume of plasma which contains N_U nuclei of uranium (all isotopes) per unit volume, $F_e(E)dE$ is the electron flux at the energy E, and $d\sigma_B(E_\gamma)/dE_\gamma$ is the cross section for Bremsstrahlung emission of photons by electrons of energy E, differential in the photon energy E_γ. The rate of formation of nuclei in the isomeric state following resonant photoabsorption that excites the nuclear state n, can then be written

$$\lambda_N=\sum_n Y_n\int_E\sigma_n^p(E)F_e(E)dE, \tag{25}$$

where the effective cross section for production of the state n via photoexcitation arising from Bremsstrahlung generated by the moving electrons is given by

$$\sigma_n^p=t_U\left(\frac{d\sigma_B(E)}{dE_\gamma}\right)_{E_\gamma=E_N}(\pi^2g\lambda_n^2\Gamma_n^\gamma), \tag{26}$$

where t_U is the target thickness in atoms per cm^{-2}.

In the case of the 500 keV electron beam of Ref. [5], the differential cross sections for production of Bremsstrahlung photons with energies of the order of 100 keV are found from [49] to be of the order of 10^{-27} cm^2 eV^{-1}. Assuming a target thickness of uranium of 20 mg cm^{-2} for the experiment of Ref. [5] gives $t_U\simeq5\times10^{19}$ atoms per cm^2. Table IV shows values of Γ_n^γ and the cross sections, σ_n^p for some low-lying transitions. Direct photoexcitation of the 77 eV level in an $E3$ transition is negligible because of the small photoexcitation width ($\simeq10^{-40}$ eV) of this transition. The largest photoexcitation cross sections again arise from 5/2+ states at 129 and 333 keV. Multiplying by the deexcitation probabilities to the 77 eV state, estimated from the branching ratios of [50] yields a total photoexcitation cross section of approximately 10^{-33} cm^2, which corresponds to a nuclear excitation rate per nucleus of the order of 10^{-7} s^{-1}. This estimate should be considered an upper estimate since no account has been taken of photon absorption in the target. The contribution of photoexcitation to nuclear excitation in the experiment [5] is thus less than that arising from inelastic electron scattering.

In the case of the laser plasma experiment [3], the Bremsstrahlung cross section estimated from [49] is 10^{-23} cm^2 eV^{-1}. Assuming a Maxwellian distribution of plasma electron energies with $kT\simeq100$ eV yields nuclear excitation rates less than 10^{-17} s^{-1}, negligible in comparison with the experimental result. Excitation rates to higher-lying nuclear states are even smaller because the probability $P(E,T)$ decreases rapidly with increasing electron energy. Thus photoexcitation can be ruled out as an explanation for the observed isomer production in the laser plasma experiment [3].

TABLE V. Summary of theoretical nuclear excitation rates (s^{-1}) per ^{235}U nucleus for three cases : a plasma with electron density $n_e = 10^{19}$ cm^{-3} and temperature $T = 100$ eV, a plasma with $n_e = 10^{19}$ cm^{-3} and $T = 20$ eV, and finally nuclear excitation resulting from interactions of beam electrons in a 500 keV electron beam with a ^{235}U target.

Conditions	NEET	NEEC	Inelastic scattering	Photoexcitation
Plasma $T = 100$ eV	$10^{-6} - 1$	10^{-11}	10^{-16}	$< 10^{-17}$
Plasma $T = 20$ eV	$10^{-9} - 10^{-4}$	10^{-11}	10^{-17}	$< 10^{-17}$
500 keV e^- beam			10^{-7}	$< 10^{-7}$

VII. CONCLUSIONS

Table V summarizes the theoretical results for excitation of ^{235m}U discussed above. These values can be compared with the experimental results shown in the last row of Table I. The largest values of the theoretical nuclear excitation rates come from the NEET process which is sensitive to the plasma temperature. At 100 eV the NEET rate is dominated by the near-resonant electronic transition $6d_{5/2} \rightarrow 6p_{1/2}$ while at 20 eV the rate is dominated by the electronic transition $6p_{1/2} \rightarrow 5d_{5/2}$. The uncertainty in the theoretical transition energies at the level of a few eV combined with the large number of possible NEET resonances arising from the many different excited states populated in the plasma has the consequence that the theoretical results for the nuclear excitation rates lie in a range spanning approximately five orders of magnitude. The revised experimental values for the nuclear excitation rate in the experiments [3] and [5] given in the bottom row of Table I lie at the upper end of the theoretical ranges. It should be noted that the theoretical estimates of NEET presented here are based on a static model of the plasma with nuclear excitation in a central hot spot defined by a single electron density and temperature. In reality, there is a continuous variation in density and temperature as the plasma plume expands away from the focal spot. Thus NEET transitions favored in the lower density plume may be different from those favored in the central dense region of the plasma. In addition NEET reactions could also occur in the conduction zone of compressed matter behind the hot spot. Errors in the experimental values for the nuclear excitation rates could result from imprecise knowledge of the plasma volume and uranium ion and electron densities. Several experimental investigations of nuclear excitation of ^{235}U in a plasma are currently in progress in order to clarify the experimental situation.

As far as other candidates for possible future experimental observation of NEET are concerned, we note that in general the NEET rate will be large when the electronic matrix elements are large, when the energy mismatch is small and when the half-life of the excited state for decay to the ground state is short. In addition, for a given multipole transition, the electronic matrix elements will be large when the nuclear charge is large and when the principal quantum numbers of the bound atomic orbitals are small since the bound electron density is then localized in the small-r region where the multipole operator is large. At the same time, it is desirable from the experimental point of view to work with a nucleus which is stable, or which has a long half-life in the ground state, and for which the isomeric state has a half-life that is sufficiently long ($t_{1/2} >$ ns) in order to permit the excited nuclei arising from the laser-irradiated target to be analyzed spectroscopically. Possible candidates include the nuclei ^{201}Hg ($M1, E_N = 1.56$ keV), ^{193}Pt ($M1, E_N = 1.64$ keV), and ^{205}Pb ($E2, E_N = 2.33$ keV).

APPENDIX: NUCLEAR ELECTROMAGNETIC MOMENTS

The nuclear electromagnetic moment for an electric multipole transition of multipolarity L is defined by [51]

$$B(EL) = \frac{1}{(2j_n+1)} |\langle j_n' || M(EL) || j_n \rangle|^2, \tag{A1}$$

where j_n and j_n' denote the nuclear spins in the initial and final state and $M(EL)$ is the nuclear electric multipole operator. For the $E3\ \frac{1}{2} + \frac{1}{2}[631] \rightarrow \frac{7}{2} - \frac{7}{2}[743]$ transition it is convenient to estimate the B value using the experimental value for the internal conversion half-life of the $\frac{7}{2}-$ state (26.8 m) and the theoretical result for the internal conversion coefficient, $\alpha = 2.5 \times 10^{20}$ obtained by interpolation of the results in [40] which were calculated using Dirac-Fock electron wave functions. The total decay rate λ_T can be expressed in terms of the internal conversion coefficient α through

$$\lambda_T = (1+\alpha)\lambda_\gamma, \tag{A2}$$

where the radiative rate λ_γ is given by

$$\lambda_\gamma = \frac{8\pi}{[(2L+1)!!]^2} \frac{L+1}{L} E_\gamma^{2L+1} B(EL). \tag{A3}$$

Using these relations, together with the values given above for α and λ_T, yields $B(\frac{1}{2}+ \rightarrow \frac{7}{2}-) = 192.5\ e^2\ \mathrm{fm}^6$. The Weisskopf model gives the following result for an electric multipole transition of multipolarity L [51]:

$$B(EL) = \frac{1.2^2 L}{4\pi} \left(\frac{3}{L+3} \right)^2 A^{2L/3} e^2 (\mathrm{fm})^{2L} = 3280\ e^2\ \mathrm{fm}^6. \tag{A4}$$

Thus the transition is hindered by a factor $H_W = 0.06$. The B value for inverse transition (from the ground state g to the excited state e) is related to that for the decay of the excited state by

$$\frac{B(g \rightarrow e)}{B(e \rightarrow g)} = \frac{(2j_n'+1)}{(2j_n+1)}. \tag{A5}$$

Thus the B value for excitation of the ground state to the isomeric level is $B(\frac{7}{2}- \rightarrow \frac{1}{2}+) = 48.1\ e^2\,\mathrm{fm}^6$.

No direct experimental information is available on the B values for $E1$ transitions from the ground state to low-lying states of ^{235}U. Here we estimate the associated B values from $B = B_W H_W$ where B_W is the Weisskopf model result and H_W is the hindrance factor. We estimate the latter using data on the related transitions in ^{239}Pu [52]. This approach gives $H_W(\frac{7}{2}-\frac{7}{2}[743] \rightarrow \frac{1}{2}+\frac{5}{2}[631]) = 1.8\times 10^{-9}$ and $H_W(\frac{7}{2}-\frac{7}{2}[743] \rightarrow \frac{5}{2}+\frac{5}{2}[622]) = 6.3\times 10^{-7}$ We then obtain the following B values for ^{235}U $E1$ transitions: $B(\frac{7}{2}-\frac{7}{2}[743] \rightarrow \frac{1}{2}+\frac{5}{2}[631]) = 4.5\times 10^{-35}\ e^2\,\mathrm{cm}^2$ and $B(^{239}\mathrm{Pu}\,\frac{7}{2}-\frac{7}{2}[743] \rightarrow \frac{5}{2}+\frac{5}{2}[622]) = 1.5\times 10^{-32}\ e^2\,\mathrm{cm}^2$. If we assume also that the hindrance factors for the transitions $\frac{7}{2}-\frac{7}{2}[743] \rightarrow \frac{5}{2}+\frac{5}{2}[633]$ and $\frac{7}{2}-\frac{7}{2}[743] \rightarrow \frac{5}{2}+\frac{5}{2}[622]$ are the same, then the B value for the $\frac{7}{2}-\frac{7}{2}[743] \rightarrow \frac{5}{2}+\frac{5}{2}[633]$ transition in ^{235}U is also equal to $1.5\times 10^{-32}\ e^2\,\mathrm{cm}^2$. The latter value may be compared with the value of $B = 2\times 10^{-32}\ e^2\,\mathrm{cm}^2$ reported in [47].

[1] S. Matinyan, Phys. Rep. **298**, 199 (1998).
[2] G. C. Baldwin and J. C. Solem, Rev. Mod. Phys. **69**, 1085 (1998).
[3] Y. Izawa and C. Yamanaka, Phys. Lett. **88B**, 59 (1979).
[4] R. V. Arutyunyan *et al.*, Kurchatov Institute of Atomic Energy Preprint IAE-4864/2 (1989).
[5] R. V. Arutyunyan, L. A. Bolshov, V. D. Vikharev, S. A. Dorshakov, V. A. Kornilo, A. A. Krivolapov, V. P. Smirnov, and E. V. Tkalya, Sov. J. Nucl. Phys. **53**, 23 (1991).
[6] J. A. Bounds and P. Dyer, Phys. Rev. C **46**, 852 (1992).
[7] M. Morita, Prog. Theor. Phys. **49**, 1574 (1973).
[8] E. V. Tkalya, Nucl. Phys. **A539**, 209 (1992).
[9] E. V. Tkalya, Sov. Phys. JETP **75**, 200 (1992).
[10] D. P. Gretouchkin and A. A. Soldatov, Kurchatov Institute of Atomic Energy - Russian Science Center Report IAE-2706 (1976).
[11] F. Karpeshin, M. R. Harston, F. Attallah, J. F. Chemin, J. N. Scheurer, I. M. Band, and M. B. Trzhaskovskaya, Phys. Rev. C **53**, 1640 (1996).
[12] F. Attallah *et al.*, Phys. Rev. Lett. **75**, 1715 (1995).
[13] F. Attallah *et al.*, Phys. Rev. C **55**, 1665 (1997).
[14] T. Carreyre *et al.* (private communication).
[15] V. I. Goldanskii and V. A. Namiot, Sov. J. Nucl. Phys. **33**, 169 (1981).
[16] N. Cue, J-C. Poizat, and J. Remillieux, Europhys. Lett. **8**, 19 (1989).
[17] J. F. Berger, D. M. Gogny, and M. S. Weiss, Phys. Rev. A **43**, 455 (1991).
[18] S. Typel and C. Leclerq-Willain, Phys. Rev. A **53**, 2547 (1996).
[19] P. Kalman and T. Keszthelyi, Phys. Rev. A **47**, 1320 (1993).
[20] G. M. Irwin and K. H. Kim, Phys. Rev. Lett. **79**, 990 (1997).
[21] D. S. Richardson, D. M. Benton, D. E. Evans, J. A. R. Griffith, and G. Tungate, Phys. Rev. Lett. **80**, 3206 (1998).
[22] S. B. Utter, P. Beiersdorfer, A. Barnes, R. W. Loughheed, J. R. Crespo Lopez-Urrutia, J. A. Becker, and M. S. Weiss, Phys. Rev. Lett. **82**, 505 (1999).
[23] F. X. Hartmann, D. W. Noid, and Y. Y. Sharon, Phys. Rev. A **44**, 3210 (1991).
[24] K. Otozai, R. Arakawa, and M. Morita, Prog. Theor. Phys. **50**, 1771 (1973).
[25] K. Otozai, R. Arakawa, and T. Saito, Nucl. Phys. **A297**, 97 (1978).
[26] A. Sinohara, T. Saito, M. Shoi, A. Yokohama, H. Baba, M. Ando, and K. Taniguchi, Nucl. Phys. **A472**, 151 (1987).
[27] T. Saito, A. Sinohara, and K. Otozai, Phys. Lett. **92B**, 293 (1980).
[28] H. Fujioka, K. Ura, A. Sinohara, T. Saito, and K. Otozai, Z. Phys. A **315**, 121 (1984).
[29] L. Lakosi, N. C. Tam, and I. Pavlicsek, Phys. Rev. C **52**, 1510 (1995).
[30] K. Pisk, Z. Kaliman, and B. A. Logan, Nucl. Phys. **A504**, 103 (1989).
[31] A. Ljubicic, D. Kekez, and B. A. Logan, Phys. Lett. B **272**, 1 (1991).
[32] H. Yukun, Z. Baohui, and Y. Zhushu, High Energy Phys. Nucl. Phys. **16**, 321 (1991).
[33] Y. Ho, B. Zhang, and Z. Yuan, Phys. Rev. C **44**, 1910 (1991).
[34] Y. Ho, Z. Yuan, B. Zhang, and Z. Pan, Phys. Rev. C **48**, 2277 (1993).
[35] N. C. Pyper, I. P. Grant, and N. Beatham, Comput. Phys. Commun. **15**, 387 (1978).
[36] J. D. Huba, NRL Plasma formulary, NRLPU-6790-98-358 (1998).
[37] D. Colombant and G. F. Tonon, J. Appl. Phys. **44**, 3524 (1973).
[38] I. P. Grant, B. J. McKenzie, P. H. Norrington, D. F. Mayers, and N. C. Pyper, Comput. Phys. Commun. **21**, 207 (1980).
[39] P. Dallot and V. Meot (private communication).
[40] I. M. Band and M. B. Trzhaskovskaya, At. Data Nucl. Data Tables **55**, 43 (1993).
[41] M. R. Harston *et al.* (unpublished).
[42] K. Alder, A. Bohr, T. Huus, B. Mottleson, and A. Winther, Rev. Mod. Phys. **28**, 432 (1956).
[43] W. C. Barber, Annu. Rev. Nucl. Sci. **12**, 1 (1962).
[44] H. Theissen, in *Springer Tracts in Modern Physics Vol. 65* (Springer, Berlin, 1972), p. 1.
[45] T. W. Donnelly and J. D. Walecka, Annu. Rev. Nucl. Sci. **25**, 329 (1975).
[46] M. Rosen, R. Raphael, and H. Uberall, Phys. Rev. **163**, 927 (1967).
[47] E. V. Tkalya, JETP Lett. **53**, 463 (1991).
[48] *The Electromagnetic Interaction in Nuclear Spectroscopy*, edited by W. D. Hamilton (North-Holland, Amsterdam, 1975), p. 37.
[49] R. H. Pratt, H. K. Tseng, C. M. Lee, L. Kissel, C. MacCallum, and M. Riley, At. Data Nucl. Data Tables **20**, 175 (1977).
[50] R. B. Firestone, *Table of Isotopes* (Wiley, New York, 1996).
[51] *The Electromagnetic Interaction in Nuclear Spectroscopy* [48], p. 149.
[52] C. F. Perdrisat, Rev. Mod. Phys. **38**, 41 (1966).